J. Phys. Chem. A **1997,** *101,* 8547−8553

Reactions of Laser-Ablated Manganese Atoms with Dioxygen. Infrared Spectra of MnO, OMnO, $Mn(O_2)$, $(MnO)_2$, and Higher Oxide Complexes in Solid Argon

George V. Chertihin and Lester Andrews*

Department of Chemistry, University of Virginia, Charlottesville, Virginia 22901

Received: June 3, 1997[⊗]

Laser-ablated Mn atoms react with O_2 to give MnO, OMnO, $(MnO)_2$, and MnO_2^- as major products, which are identified from oxygen isotopic substitution on their matrix infrared spectra. Annealing allows further association to form the cyclic $Mn(O_2)$ complex, $(O_2)MnO$ and $(O_2)MnO_2$ oxide complexes, and higher oxides. The OMnO molecule is bent based on the observation of both ν_3 and ν_1 and on DFT calculations; the oxygen-18 shift for ν_3 provides a valence angle determination of 135 ± 5°. The cyclic $Mn(O_2)$ molecule involves a weaker bonding interaction than the cyclic $Fe(O_2)$ molecule. The short 2.6 Å estimated Mn−Mn distance across the rhombic $(MnO)_2$ ring is compatible with substantial metal−metal bonding.

Introduction

The present work is devoted to investigation of the manganese−oxygen system and continues our systematic study of laser-ablated transition metal atom reactions with small molecules. Manganese is of chemical interest due to its wide application in catalysis and in solid state and alloy materials.[1,2] Among the oxides more work has been done on the MnO molecule, which has been investigated in the gas phase by ab initio calculations and by matrix ESR.[3−7] Higher manganese oxides have been observed in matrix isolation studies,[7−11] including $Mn(O_2)$, MnO_2, MnO_3, MnO_4, and Mn_2O_7; however, the ESR and IR investigations on OMnO presented contradictory results. The electron spin resonance spectrum suggested a linear OMnO molecule,[7] while infrared work assigned 950 and 898 cm^{-1} bands to stretching vibrations of bent OMnO and also found a cyclic $Mn(O_2)$ isomer.[8,9] This discrepancy and our observation[12] of bent OFeO as the major reaction product using laser-ablated Fe atoms prompted a reinvestigation of the Mn + O_2 system. Moreover, laser-ablated metal atoms lead to different initial reaction products and result in much richer chemistry than ordinary thermal evaporation experiments.[12] This is in part due to the formation of metastable states, which have been extensively studied[13] for Mn and can serve to activate chemical reactions. The manganese−oxygen system is interesting for comparison of transition metal chemistry and metal oxide structure with previous work on iron and chromium in this laboratory.[12,14]

Experimental Section

The technique for laser ablation and FTIR matrix investigation has been described previously.[12,14] Manganese (Johnson Matthey, 99.99%) was mounted on a rotating (1 rpm) stainless steel rod. The Nd:YAG laser fundamental (1064 nm, 10 Hz repetition rate, 10 ns pulse width) was focused on the target through a hole in the CsI cryogenic (10 K) window. Laser power ranged from 20 to 40 mJ/pulse at the target. Metal atoms were co-deposited with 0.25−1% O_2 (and isotopic modifications) in argon or nitrogen at 2−4 mmol/h for 1−2 h periods. FTIR spectra were recorded with 0.5 cm^{-1} resolution on a Nicolet 750. Matrix samples were temperature cycled, and more spectra were collected; selected samples were subjected to broadband photolysis by a medium-pressure mercury arc (Philips, 175 W) with globe removed (240−580 nm).

Results

The laser-ablated Mn + O_2 reaction products trapped in solid argon will be presented; infrared spectra are shown in Figure 1 and absorptions are listed in Table 1. The most intense new bands observed after deposition were 953.0, 948.0, 858.2, 847.3, 833.1, 816.4, 808.3, 601.0, and 505.0 cm^{-1}. Photolysis increased the 948.0 and 816.4 cm^{-1} bands, decreased the 858.2 and 833.1 cm^{-1} absorptions, and almost destroyed the 847.3 and 808.3 cm^{-1} bands, leaving other absorptions unchanged. Annealing produced a complex set of new absorptions, most notably at 1108.2, 1092.2, 974.9, 951.4, 886.9, 850.7, and 686.4 cm^{-1}; the 948.0, 858.2, 833.1, 816.4, 601.0, and 501.0 cm^{-1} bands decreased, which is shown in Figure 1. Increasing oxygen concentration led to a relatively higher yield of the 974.9, 951.4, 948.0, and 816.4 cm^{-1} bands; increasing laser power enhanced the intensity of all bands and increased the 847.3, 808.3, 603.9, and 506.8 cm^{-1} bands relative to the 833.1 cm^{-1} band.

Oxygen isotopic substitution was employed for band identification. The observed isotopic patterns, for mechanical ($^{16}O_2$ + $^{18}O_2$) and statistical ($^{16}O_2$ + $^{16}O^{18}O$ + $^{18}O_2$) mixtures will be discussed in the next section. Figures 2 and 3 show important spectral regions.

A complementary experiment was done with 0.5% N_2O in argon. After deposition the most intense bands were 987.7, 868.5, and 833.1 cm^{-1}. Weak 960.5, 948.0, 813.2, and 808.3 cm^{-1} bands were also observed. The 987.7, 960.5, and 868.5 cm^{-1} bands increased, the 948.0 and 833.1 cm^{-1} bands decreased, and a weak 847.3 cm^{-1} band appeared on annealing. No 601.0, 505.0 cm^{-1} bands were detected.

Reactions were performed with O_2 in N_2 matrixes, and the product absorptions are listed in Table 2. New absorptions for MnN and $Mn(N_2)_x$ will be described in a separate report. The major new features are a doublet at 969.6, 964.4 cm^{-1}, a sharp 866.7 cm^{-1} band, a broad 843.8 cm^{-1} band with a sharp 841.8 cm^{-1} shoulder, and a strong 538.3 cm^{-1} feature.

Density functional theory (B3LYP) calculations using the GAUSSIAN 94 program[15] and 6-311G* and 6-311+G* basis sets for Mn and O atoms were performed for all isomers of MnO_2, and results are listed in Table 3. For bent OMnO, doublet and quartet states were found, and the quartet is the most stable, in agreement with ESR results.[7] For cyclic Mn-

---

[⊗] Abstract published in *Advance ACS Abstracts,* October 1, 1997.

S1089-5639(97)01813-6 CCC: $14.00 © 1997 American Chemical Society

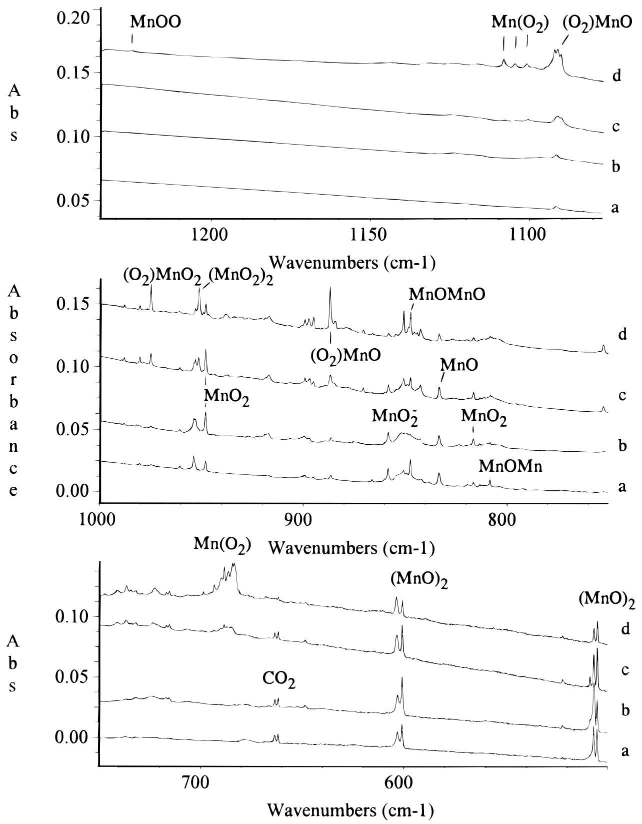

Figure 1. Infrared spectra of laser-ablated Mn atoms co-deposited with O_2 in excess argon at 10 ± 1 K: (a) 0.5% O_2 co-deposited sample, (b) after broadband photolysis for 30 min, (c) after annealing to 25 K, and (d) after annealing to 35 K.

(O_2), doublet, quartet, and sextet states were converged with the first basis set and only doublet and quartet states with the second set. For bent MnOO, quartet and sextet states were found with the first and only sextet with the second basis set. The calculated relative stabilities of these isomers is also shown in Table 3. The DFT calculations are reliable only for the OMnO molecule, as both basis sets produced the same electronic states with the same relative energies. The large basis set gave better frequencies in comparison with experiment. Unfortunately, for cyclic Mn(O_2) the frequency agreement is not good. Different electronic states and different energy separations were obtained for each basis set. Obviously, higher levels of theory must be employed including electron correlation and configuration interaction.

Discussion

The assignment of manganese oxide spectral bands will be presented.

MnO. The 833.1 cm^{-1} band was observed after deposition. It decreased on annealing and photolysis and produced doublets with both mechanical and statistical isotopic mixtures. The 16/18 isotopic ratio (1.0457) is very close to the theoretical harmonic diatomic ratio (1.0461). This band is assigned to the diatomic MnO molecule, in good agreement with the gas-phase value ($\Delta G_{1/2} = 830.0$ cm^{-1}).[3] Similar small matrix shifts have been observed for FeO, CoO, and NiO in solid argon.[12,16-18]

The strong 868.5 cm^{-1} band was observed after deposition with the N_2O/Ar mixture. Although it is hard to make a definitive assignment without isotopic substitution, high absorbance in the N_2O system, growth on annealing, and blue shift from the MnO allow assignment of this band to the NNMnO complex by comparison with the Fe + O_2 system.[12]

Previous infrared experiments failed to observe MnO using thermal evaporation of Mn and O_2, H_2O, H_2O_2, and N_2O oxidizers.[7-9,20-22] However, ESR work produced this molecule in reactions with O_2 and N_2O after strong vacuum ultraviolet photolysis, although the yield was small, and only the reaction with ozone gave high yield.[7] Heat changes for the reactions Mn + X (X = O_2, H_2O, N_2O, H_2O_2, and O_3) are estimated as follows:[3]

$$\mathrm{Mn} + \mathrm{O_2} \rightarrow \mathrm{MnO} + \mathrm{O} \qquad \Delta H = +33\ \mathrm{kcal/mol} \qquad (1)$$

$$\mathrm{Mn} + \mathrm{H_2O} \rightarrow \mathrm{MnO} + \mathrm{H_2} \qquad \Delta H = +32\ \mathrm{kcal/mol} \qquad (2)$$

$$\mathrm{Mn} + \mathrm{N_2O} \rightarrow \mathrm{MnO} + \mathrm{N_2} \qquad \Delta H = -45\ \mathrm{kcal/mol} \qquad (3)$$

$$\mathrm{Mn} + \mathrm{H_2O_2} \rightarrow \mathrm{MnO} + \mathrm{H_2O} \qquad \Delta H = -52\ \mathrm{kcal/mol} \qquad (4)$$

$$\mathrm{Mn} + \mathrm{O_3} \rightarrow \mathrm{MnO} + \mathrm{O_2} \qquad \Delta H = -59\ \mathrm{kcal/mol} \qquad (5)$$

The first two reactions are endothermic and obviously cannot lead to spontaneous MnO formation. Reactions 3 and 4 are exothermic, but they probably have high activation barriers, and only the most exothermic reaction (5) produced sufficient MnO for the ESR detection.[7] In our experiments MnO was the first product of reactions 1 and 3, which demonstrates the reactivity of energetic laser-ablated Mn atoms.[13]

MnO_2, OMnO. New bands at 948.0 and 816.4 cm^{-1} appeared in the spectra after deposition even with threshold laser power. These bands decreased on annealing, while photolysis doubled their intensities. Both bands produced doublet structures with the mechanical mixture (Figure 2) and triplet isotopic structures with scrambled isotopic oxygen (Figure 3), which indicates that this product contains two equivalent oxygen atoms. Appearance in low laser power experiments also suggests a one manganese atom primary reaction product. The 16/18 ratios 1.0389 and 1.0530 are characteristic of antisymmetric and symmetric vibrations of a bent symmetrical triatomic molecule. The matching of asymmetries in the triplets (the $^{16}OMn^{18}O$ components are up and down 2.6 ± 0.1 cm^{-1} from the averages of $^{16}OMn^{16}O$ and $^{18}OMn^{18}O$ components for ν_3 and ν_1, respectively) further associates the 948.0 and 816.4 cm^{-1} bands with the same molecule. Thus, these bands are assigned to the bent manganese dioxide molecule. The upper limit of valence angle estimated from the ν_3 isotopic ratio is 140 ± 5°, which is in good agreement with the previous IR work,[8,9] but in disagreement with the ESR investigation, which concluded that OMnO is linear.[7] Clearly, the ESR spectrum is not sensitive to a small departure from linearity for this quartet state dioxide molecule.

The present DFT calculations with two different basis sets gave 131° for the $^4B_1$ ground state. In the case of OFeO, a similar DFT calculation gave 141° for the ground triplet state, and upper limit−lower limit determinations from the 16/18 and 54/56 isotopic ratios were 158 ± 5° and 144 ± 5°.[12] From such observations, the OFeO valence angle was determined to be 150 ± 10°. For the OCrO molecule, a similar DFT calculation predicted 125° for the $^3B_1$ ground state, and 16/18 and 52/53 isotopic ratios yielded 128 ± 4°.[14] The present infrared spectrum and DFT calculations on OMnO predict a 135 ± 5° valence angle for OMnO. The bond dipole model[23] can be used to estimate valence angle from the relative intensities of ν_1 and ν_3 observed here (3 to 10). This predicts a valence angle of 123°, in reasonable agreement with the above values.

In addition, the main discrepancy with the previous IR work is the ν_1 assignment. The previously assigned 898 cm^{-1} band was also observed in our experiments, but it appears in the spectra after annealing, and its behavior does not correlate with the strong ν_3 band at 948.0 cm^{-1}. Moreover, a 526 cm^{-1} band was also previously assigned to the bending mode of OMnO,

TABLE 1: Infrared Absorptions (cm^{-1}) Observed for Reactions of Laser-Ablated Mn Atoms and O_2 Molecules during Condensation in Excess Argon at 10 K

$^{16}O_2$	$^{18}O_2$	$^{16}O_2 + {}^{16}O^{18}O + {}^{18}O_2$	*R* (16/18)	anneal[a]	assignment
1509.0	1423.8	1509.0, 1467.0, 1423.9	1.0598	+	$Mn_x(O_2)$
1230.2 br	1161.6 br		1.0591	+	MnOO site
1224.5	1156.5		1.0588	+	MnOO
1130 br	1066 br		1.060		$(O_2)MnO_2$
1108.2	1046.1	1108.2, 1077.9, 1046.1	1.0594	++	$Mn(O_2)$
1104.8	1042.5	1104.8, 1074.4, 1042.5	1.0598	++	$Mn(O_2)$
1100.8	1039.2	1100.8, 1070.3, 1039.2	1.0593	++	$Mn(O_2)$
1094 sh	1033 sh	1065 sh	1.059	+	site
1092.2	1030.7	1062.0	1.0597	++	$(O_2)MnO$
1090.2	1028.8	1060.0	1.0597	++	$(O_2)MnO$
987.8	951.0		1.0387	+	N_2-MnO_2
980.3	942.6	980.3, 968.8, 942.6	1.0400	+	$(O_2)MnO_2$ site
974.9	937.5	974.9, 963.5, 937.5	1.0399	++	$(O_2)MnO_2$ (ν_3)
960.5	924.3	*960.5*, *945.3*, *924.3*[b]	1.0392	−	OMnO site
953.8	901.8	sextet	1.0576		O_4^-
953.0	917.3	*953.0*, 937.9, *917.2*	1.0389	−	OMnO site[c]
951.4	907.6	*951.4*, *945.3*, 944.7, 938.7, *933.1*, 925.9, 912.9, *907.6*	1.0483	++	$(MnO_2)_2$
948.0	912.5	*948.0*, 932.9, *912.5*	1.0389	+, −	OMnO (ν_3)
917.0	879.3		1.0429	+, −	Mn_xO_y
897.1	862.6	896.9, 862.7	1.0400	+, −	Mn_xO_y
895.1	851.6		1.0511	+	Mn_xO_y
886.9	847.3	886.4, 847.9, 847.3	1.0467	++	$(O_2)MnO$
858.2	826.2	*858.2*, 845.6, *826.2*	1.0389	−	MnO_2^- (ν_3)
850.7	809.7	850.7, 849.3, 809.7	1.0506	+	(OMnOMnO)
847.3	808.7	847.9, *847.3*, *808.7*, 808.1	1.0476	+	MnOMnO
842.4	805.6		1.0456	+	MnO site
833.1	796.7		1.0457	−	MnO
816.4	775.3	816.4, 793.3, 775.3	1.0530	+, −	OMnO (ν_1)
813.2	773.4	813.2, 773.4	1.0515	−	MnOMn site
808.3	768.7	808.3, 768.7	1.0515	+, −	MnOMn
752.3	718.1		1.0476	+	Mn_xO_y
736.4	705.7		1.0435	+	Mn_xO_y
723.3	689.6		1.0489	+	Mn_xO_y
688.6	661.6	688.6, 676.1, 661.6	1.0408	++	$Mn(O_2)$
686.4	659.9	686.4, 673.9, 659.9	1.0402	++	$Mn(O_2)$
683.9	657.6	683.9, 671.3, 657.6	1.0400	++	$Mn(O_2)$
603.9	574.2	603.9, 621.2, 583.7, 577.2	1.0463	+	site
601.0	577.7	601.0, 618.6, 581.2, 574.7	1.0458	+	$(MnO)_2$
506.8	484.5	506.8, 496.8, 484.5	1.0460	+	$(MnO)_2$
505.0	482.7	505.0, 495.1, 482.7	1.0462	+	site

[a] Annealing behavior: ++ increased markedly, + increased, − decreased. [b] Italic OMnO bands observed in $^{16}O_2 + {}^{18}O_2$ experiment. [c] Produced by broadband photolysis.

but this band was not observed here, and no bands below 600 cm^{-1} in our experiments can be connected with the dioxide based on isotopic substitution, annealing, and photolysis behavior.

Two weaker bands at 960.5 and 953.0 cm^{-1} exhibit essentially the same 16/18 ratios and triplet statistical mixed isotopic patterns and are thus due to minor matrix sites of OMnO. These slightly different matrix site absorptions are formed primarily by different mechanisms, as will be discussed below.

The strong doublet at 969.6, 962.4 cm^{-1} in solid nitrogen was observed after deposition and decreased on annealing. Isotopic substitution revealed doublet and triplet structures with mechanical and statistical isotopic mixtures, respectively, with the 16/18 ratio 1.0393/1.0384. This band is assigned to the ν_3 vibration of the OMnO molecule in solid N_2; the weaker ν_1 counterpart was not found in N_2 experiments.

In matrix isolation studies of the photochemistry of $Mn_2(CO)_{10}$ in the presence of 5% O_2 in solid argon,[11] the major product was identified as Mn_2O_7 by comparison with a spectrum of the authentic material.[10] The photolysis product at 952 cm^{-1} was, however, noted to be substantially more intense than product bands in this spectrum at 783 and 767 cm^{-1}, which correspond to the strongest absorption reported for Mn_2O_7 and assigned to the antisymmetric Mn−O−Mn stretching mode.[10] The present work strongly suggests that most of the 963, 956, 952 cm^{-1} product band in the photolysis work[11] is in fact due to OMnO (slightly perturbed by interaction with other molecules such as CO and O_2 present in the matrix, as has been found for CrO_2 as well[14]), while the weaker bands may well be due to Mn_2O_7, as assigned.[11] Thus the lower oxidation state OMnO molecule is probably the major photolysis product.

$Mn(O_2)$. The split band at 688.6, 686.4, 683.9 cm^{-1} always appeared in the spectra after 25 K annealing and increased markedly on annealing to higher temperatures. Oxygen isotopic substitution revealed doublet and triplet isotopic structures with mechanical and statistical mixtures, respectively, and 16/18 isotopic ratios near 1.040. On the basis of annealing behavior and isotopic data this band must be considered for the cyclic $Mn(O_2)$ molecule. An estimation of the isotopic ratio for ν_2 of $Mn(O_2)$ (neglecting off-diagonal terms in the **G** matrix and assuming a 40° angle) gives 1.039. Strong ν_2 vibrations have been observed for group alkali cyclic metal oxides, and the $M^+(O_2)^-$ ionic structure was suggested;[24] however, the near agreement between argon and nitrogen matrix observations argues against an ionic molecule here.

The sharp group of bands near 1108.2 cm^{-1} behaved similarly on annealing. Isotopic substitution gave two sharp sets of bands with the mechanical mixture and three sharp sets with the statistical mixture (Figures 2 and 3). The 16/18 ratio 1.0594 is suitable for the O−O stretching vibration, and this group is assigned to the ν_1 mode of $Mn(O_2)$. Moreover, experiments with the O_2/N_2 mixture and isotopic modifications found similar

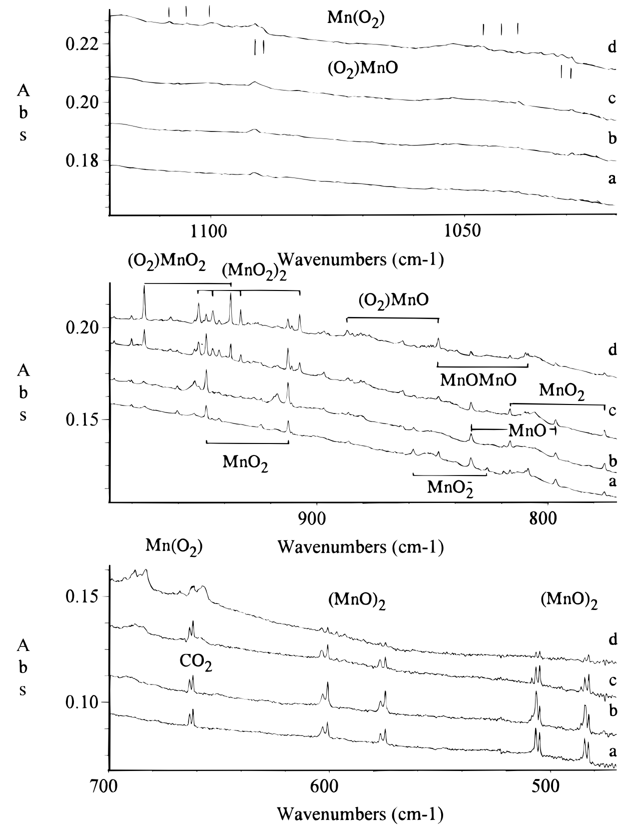

Figure 2. Infrared spectra of laser-ablated Mn atoms co-deposited with mechanical isotopic oxygen mixture in excess argon at 10 ± 1 K: (a) 0.5% $^{16}O_2$ + 0.5% $^{18}O_2$, (b) after broadband photolysis for 30 min, (c) after annealing to 25 K, and (d) after annealing to 35 K.

groups of bands around 686.6 and 1108.4 cm^{-1}, which also appeared in the spectra only after annealing, and produced doublet and triplet isotopic structures with mechanical and statistical mixtures; their 16/18 ratios (1.0412 and 1.0590) almost coincide with the argon values.

Assignment of the 1108 and 686 cm^{-1} bands to cyclic Mn(O$_2$) is in agreement with Serebrennikov,[8,9] but not with the present DFT calculations and with the adjacent cyclic Fe(O$_2$) molecule. The Mn(O$_2$) bands share with Fe(O$_2$) the substantial growth on annealing, but Fe(O)$_2$ is red shifted 37 cm^{-1} by the nitrogen matrix,[12,19] whereas Mn(O$_2$) is not shifted between argon and nitrogen. Recall that Fe(O$_2$) exhibited a strong ν_1 mode at 956 cm^{-1} and a weak ν_2 mode at 548 cm^{-1}.[12] Although matrix site splittings complicate the issue, ν_2 of cyclic Mn(O$_2$) at 686 cm^{-1} is at least 5-fold stronger than ν_1 at 1108 cm^{-1} in the infrared spectrum. The lowest cyclic state ($^4B_1$) has a calculated ν_1 at 1021 cm^{-1}, which is some 80 cm^{-1} lower than observed, but the calculated ν_2 is 235 cm^{-1} lower and the intensity much weaker than observed. We must conclude that although DFT calculations[12,18] worked very well for Fe(O$_2$) and Ni(O$_2$), a higher level of theory is needed to describe the cyclic Mn(O$_2$) molecule. The bonding interaction between Mn or Fe and dioxygen in the cyclic M(O$_2$) molecules is clearly different.

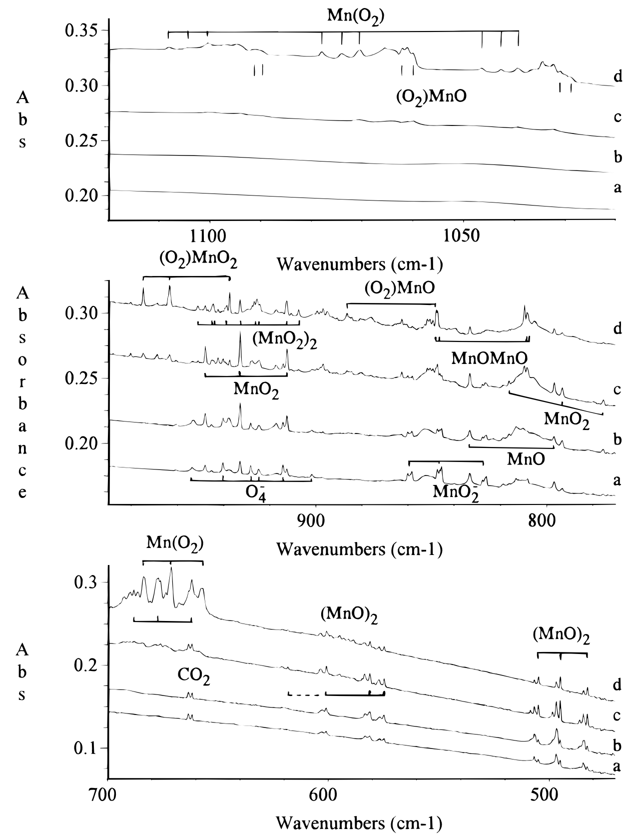

Figure 3. Infrared spectra of laser-ablated Mn atoms co-deposited with statistical isotopic oxygen mixture in excess argon at 10 ± 1 K: (a) 0.06% $^{16}O_2$ + 0.12% $^{16}O^{18}O$ + 0.06% $^{18}O_2$, (b) after broadband photolysis for 30 min, (c) after annealing to 25 K, and (d) after annealing to 35 K.

TABLE 2: Infrared Absorptions (cm^{-1}) Observed for Reactions of Laser-Ablated Mn Atoms and O$_2$ Molecules during Condensation in Excess Nitrogen at 10 K

$^{16}O_2$	$^{18}O_2$	$^{16}O_2$ + $^{16}O^{18}O$ + $^{18}O_2$	R (16/18)	anneal[a]	assignment
2100	2100	2100		+	Mn(N$_2$)$_x$
1108.4	1046.2	1108.4, 1077.9, 1046.2	1.0595	++	Mn(O$_2$)
1104.4	1042.4	1104.4, 1073.9, 1042.4	1.0596	+	Mn(O$_2$)
1095.0 w	1033.4 w		1.0596	+	?
1053.5	1053.5	1053.5		+	MnN
1043.1	985.6	sextet	1.0583	−	O$_3$
990.8 w	936.2 w		1.0583	−	O$^-{}_4$
969.6	932.9	*969.6*, 956.6, *932.4*	1.0393	−	OMnO(ν_3)
962.4	926.4	*954.4*, 949.5, *926.5*	1.0389	−	OMnO(ν_3)
866.7	834.0	*866.7*, 853.8, *834.0*	1.0392	−	MnO$^-{}_2$(ν_3)
843.8	807.1	843.8, 807.1	1.0455	−	(N$_2$)$_x$MnO
841.8	803.8	841.8, 803.8	1.0473	+	OMnOMnO
792.4	748.2		1.0592	−	O$_3^-$
686.6	659.4	686.6, 677.6, 659.4	1.0412	++	Mn(O$_2$)
685.3	658.1		1.0413	+	Mn(O$_2$)
603.2 w	576.9 w	622.8, *603.2*, 580.8, *576.9*	1.0456	−	(MnO)$_2$
538.3	515.6	*538.3*, 528.4, *515.6*	1.0440	+	(N$_2$)$_x$(MnO)$_2$
508.8	508.8	508.8		+	Mn(N$_2$)$_x$
452.4	452.4	452.4		−	Mn(N$_2$)$_x$
449.5	449.5	449.5		+	Mn(N$_2$)$_x$

[a] Annealing behavior: + increased, − decreased. [b] Italic OMnO bands observed in $^{16}O_2$ + $^{18}O_2$ experiment.

MnOO. A very weak doublet at 1230.2, 1224.5 cm^{-1} appeared in the spectra only after annealing. Due to its weakness only ^{18}O-counterparts were detected, which gave the 16/18 ratios 1.0591/1.0588. These ratios are very close to the pure oxygen diatomic ratio 1.0607; thus end-bonded manganese dioxide must be considered. On the basis of frequency prediction of DFT calculations (Table 3) and comparison with Cr, Fe, Co, and Ni + O$_2$ systems this doublet is tentatively assigned to the end-bonded MnOO molecule.[12,14,17,18] Like iron, three manganese dioxygen species have been identified, the bent dioxide OMO, the end-bonded MOO species, and the cyclic M(O$_2$) complex; however, the Mn(O$_2$) complex involves a weaker interaction with O$_2$ than the Fe(O$_2$) complex.

Reaction Mechanisms. The major OMnO absorptions were produced on sample deposition and decreased on annealing, while the Mn(O$_2$) and MnOO bands appeared. Moreover, experiments with the mechanical isotopic mixture found only

TABLE 3: Calculated (B3LYP, 6-311G*, and 6-311+G*) Geometries, Vibrational Frequencies (cm^{-1}), and Intensities (km/mol) for MnO_2 Isomers

molecule (6-311G*)	geometry (Å, deg)	$\nu_1(I)$	$\nu_2(I)$	$\nu_3(I)$
^{16}OMn^{16}O ^{4}B$_1$, 0 kcal/mol	R(Mn−O) = 1.581, α = 131°	947(53)	267(34)	1070(188)
^{16}OMn^{18}O		919(54)	261(33)	1053(179)
^{18}OMn^{18}O		899(50)	255(31)	1029(175)
^{16}OMn^{16}O ^{2}B$_1$, +12 kcal/mol	R(Mn−O) = 1.564, α = 127°	1035(37)	286(22)	1101(292)
^{16}OMn^{18}O		1002(54)	280(21)	1086(265)
^{18}OMn^{18}O		983(35)	273(20)	1058(272)
Mn(^{16}O$_2$), ^{4}B$_1$, +47 kcal/mol	R(Mn−O) = 1.829, R(O−O) = 1.396, α = 45°	1021(44)	451(1)	451(6)
Mn(^{16}O^{18}O)		993(41)	449(2)	433(4)
Mn(^{18}O$_2$)		964(39)	434(1)	427(6)
Mn(^{16}O$_2$), ^{6}B$_2$, +49 kcal/mol	R(Mn−O) = 1.915 R(O−O) = 1.367, α = 42°	1093(37)	368(30)	234(6)
Mn(^{16}O^{18}O)		1062(35)	362(29)	227(6)
Mn(^{18}O$_2$)		1031(33)	355(28)	221(5)
Mn(^{16}O$_2$), ^{2}B$_1$, +84 kcal/mol	R(Mn−O) = 1.852 R(O−O) = 1.323, α = 42°	1163(131)	364(23)	307(4)
Mn(^{16}O^{18}O)		1131(123)	358(22)	299(4)
Mn(^{18}O$_2$)		1097(115)	351(22)	291(3)
Mn^{16}O^{16}O, ^{4}A″, +47 kcal/mol	R(Mn−O) = 1.953, R(O−O) = 1.281, α = 120°	1181(831)	332(29)	191(16)
Mn^{16}O^{18}O		1145(789)	331(29)	185(14)
Mn^{18}O^{16}O		1150(778)	317(26)	188(15)
Mn^{18}O^{18}O		1113(737)	316(27)	183(14)
Mn^{16}O^{16}O, ^{6}A″, +52 kcal/mol	R(Mn−O) = 1.951, R(O−O) = 1.308, α = 111°	1130(369)	442(0)	136(3)
Mn^{16}O^{18}O		1096(350)	441(0)	132(3)
Mn^{18}O^{16}O		1100(348)	422(0)	135(3)
Mn^{18}O^{18}O		1065(328)	421(0)	130(3)

molecule (6-311+G*)	geometry (Å, deg)	$\nu_1(I)$	$\nu_2(I)$	$\nu_3(I)$
^{16}OMn^{16}O ^{4}B$_1$, 0 kcal/mol	R(Mn−O) = 1.596, α = 131°	888(52)	243(21)	995(164)
^{16}OMn^{18}O		862(52)	238(20)	979(156)
^{18}OMn^{18}O		844(48)	232(19)	957(153)
^{16}OMn^{16}O ^{2}B$_1$, +16 kcal/mol	R(Mn−O) = 1.574, α = 144°	999(19)	212(47)	1037(392)
^{16}OMn^{18}O		963(66)	207(45)	1027(331)
^{18}OMn^{18}O		946(18)	203(43)	998(364)
Mn(^{16}O$_2$), ^{4}B$_1$, +58 kcal/mol	R(Mn−O) = 1.851, R(O−O) = 1.390, α = 44°	1020(68)	393(4)	390(0)
Mn(^{16}O^{18}O)		991(64)	391(3)	375(1)
Mn(^{18}O$_2$)		962(60)	379(3)	369(0)
Mn(^{16}O$_2$), ^{2}B$_1$, +96 kcal/mol	R(Mn−O) = 1.786 R(O−O) = 1.393, α = 46°	980(166)	548(2)	408(12)
Mn(^{16}O^{18}O)		953(157)	538(2)	454(12)
Mn(^{18}O$_2$)		926(148)	527(2)	443(11)
Mn^{16}O^{16}O, ^{6}A′, +54 kcal/mol	R(Mn−O) = 1.878, R(O−O) = 1.314, α = 137°	1191(26)	460(63)	113(1)
Mn^{16}O^{18}O		1160(18)	454(62)	110(1)
Mn^{18}O^{16}O		1155(22)	446(58)	110(1)
Mn^{18}O^{18}O		1123(19)	441(58)	107(1)

doublet structures for the major site antisymmetric and symmetric vibrations of OMnO with no ^{16}OMn^{18}O. The 945.3 cm^{-1} intermediate component of the minor OMnO site was observed with half the 960.5 cm^{-1} band intensity, and photolysis produced only 953.0, 917.3 cm^{-1} for the broader site absorption. In the N_2O experiment, with a large MnO band intensity, annealing increased the 960.5 cm^{-1} band (×2) but decreased the 948.0 cm^{-1} band, and photolysis failed to produce the 953.0 cm^{-1} band.

Here we have three different mechanisms for formation of OMnO, and each is the dominant role for one of the three different site absorptions. On deposition with laser-ablated Mn atoms probably rich in ^{8}P metastable states,[13] the direct insertion into O_2 takes place followed by relaxation on collisions with condensing argon atoms. In YAG laser studies using similar ablation conditions, Levy measured velocities from 2000 to 20 000 m/s and determined $^8P_{7/2}$ and $^8P_{5/2}$ lifetimes of 82 ± 10 and 122 ± 14 μs, respectively.[13] Even with the slower velocity, Mn metastables can travel on the order of 20 cm. Although we cannot measure the argon pressure between the spray-on line and the 10 K window, the residual argon pressure 8 cm from the cold window is 10^{-4} Torr during deposition. If the average argon pressure between the target and cold window is less than 10^{-3} Torr, the mean free path is greater than 7 cm. Since the target is on the order of 2 cm from the cold window, many of the metastable Mn* atoms survive to undergo chemical reactions on the matrix surface during sample condensation. The strongest product band at 948.0 cm^{-1} is assigned to OMnO produced by direct insertion reaction 6. The broader 953.0 cm^{-1} band is weak on sample deposition, but grows markedly on broadband photolysis, while the 948.0 cm^{-1} band absorbance doubles. Clearly, reaction 6 can be initiated by broadband photoexcitation of Mn, possibly followed by relaxation to the ^{8}P metastable states at about 2.3 eV.[13] Finally, growth of the 945.3 cm^{-1} mixed isotopic band on annealing to 25 K in the $^{16}O_2 + {}^{18}O_2$ experiment, along with growth of the 960.5 cm^{-1} band in N_2O experiments with MnO and a little O_2 present, shows that this OMnO site can be formed by the reaction of O and MnO in the cold matrix.

$$\mathrm{Mn}^* + \mathrm{O}_2 \rightarrow \mathrm{OMnO} \qquad (6)$$

The $Mn(O_2)$ and MnOO molecules are formed on annealing from the reaction of cold reagents in the matrix, reaction 7. As in the case of $Fe(O_2)$, the cyclic $Mn(O_2)$ isomer is favored on annealing.

$$\mathrm{Mn} + \mathrm{O}_2 \rightarrow \mathrm{MnOO\ and\ Mn(O_2)} \qquad (7)$$

Finally, the OMnO molecule was also observed from the reaction of O_2 with thermal Mn atoms.[7,8] Probably, the activation barrier for reaction 6 is not high, and the energy of thermal Mn atoms is enough for insertion; however, the high reactivity for Mn atoms observed here is clearly due in part to the population of metastable states in laser-ablated Mn atoms.[13]

MnO_2^-. The 858.2 cm^{-1} band was observed after deposition with relatively high laser power and low oxygen concentration and decreased on annealing and photolysis. Doublet and triplet isotopic structures were found in experiments with mechanical and statistical mixtures, respectively, indicating two equivalent oxygen atoms. The 16/18 ratio 1.0387 is very close to that for the antisymmetric vibration of the bent dioxide molecule, and this product probably contains the bent OMnO fragment. On the basis of these results this band is assigned to the negative ion MnO_2^-. The isotopic ratio indicates that the geometry of OMnO does not change significantly upon electron attachment. The decrease of frequency is due to one additional electron in an antibonding orbital. Anion species have been observed in a number of laser-ablated metal atom studies in this lab.[12,25] In particular the yield of O_4^- was high in the Mn studies, indicating the availability of electrons for capture and supporting the identification of MnO_2^- in the present experiments.

In nitrogen matrixes the 866.7 cm^{-1} band appeared in the spectra after deposition and decreased on annealing. Again doublet and triplet isotopic structures were found in experiments with mechanical and statistical mixtures, and the 16/18 ratio is 1.0392. This band is due to MnO_2^- isolated in solid N_2. Another possible assignment could be the $NMnO_2$ molecule, as the analogous molecules were found for Fe and Co.[17,19] Experiments with isotopic nitrogen are required to make this assignment more definitive.

$(O_2)MnO$. The 886.9 cm^{-1} band was also observed in the spectra after annealing. It produced a doublet with both isotopic mixtures, but instead of the 886.9 and 847.3 cm^{-1} (^{18}O-counterpart) bands two new shifted 886.5 and 847.9 cm^{-1} bands were observed, which indicates a secondary isotopic splitting. The 16/18 ratio 1.0467 is very close to the harmonic diatomic value. In the upper region the matrix-split 1092.2 cm^{-1} band also appeared on annealing and behaved similarly. It produced a doublet with the mechanical mixture and a triplet with statistical isotopic oxygen and the 16/18 isotopic ratio 1.0597, and due to broadness, no secondary splitting was observed. On the basis of isotopic ratios and the appearance of small isotopic splittings, these bands are assigned to terminal Mn−O and cyclic O−O stretching vibrations of the $(O_2)MnO$ molecule. The secondary splitting of the low-frequency band is due to interaction between the terminal oxygen and cyclic O_2 group. The alternative OOMnO structure should also be considered, but the triplet structure of the upper band is more appropriate for the side-bonded molecule, as a quartet should be observed for the O−O stretching vibration of OOMnO. This is expected above 1230 cm^{-1}, as found for OONiO.[18] The $(O_2)MnO$ molecule is analogous to $(O_2)FeO$ in that the FeO fundamental is blue shifted 55.3 cm^{-1} in the complex,[12] whereas for (O_2)-MnO the MnO fundamental is blue shifted 53.8 cm^{-1} in the complex. The $(O_2)MnO$ complex characterized here could be the same MnO_3 molecule identified by ESR but it is difficult to be certain.[7] The $(O_2)MnO$ molecule is formed by reaction 8, which does not require activation energy.

$$O_2 + MnO \rightarrow (O_2)MnO \tag{8}$$

$(MnO)_2$. Two doublets at 603.9/601.0 and 506.8/505.0 cm^{-1} were also observed after deposition and decreased on annealing. Both doublets produced doublet isotopic structures in experiments with the mechanical mixture and the 16/18 ratios 1.0458 and 1.0462, which are very close to the harmonic diatomic ratio. With statistical isotopic oxygen, the first band produced a highly asymmetric triplet (the central component was shifted down from the center of gravity) and the new band 621.1, 618.8 cm^{-1}, while the second band produced a triplet absorption. This region is appropriate for the bridged M−O−M vibrations, and both doublets are assigned to the B_{2u} and B_{3u} vibrations of the rhombus $(MnO)_2$ molecule. The appearance of the new doublet in the statistical oxygen experiments is due to the symmetric vibration of the isotopically mixed $Mn_2{}^{16}O^{18}O$ molecule, which interacts strongly with the antisymmetric vibration. Analogous rhombic transition metal oxide dimer molecules have been characterized for Fe, Co, and Ni with observation of both B_{2u} and B_{3u} stretching modes.[12,17,18] The O−Mn−O angle can be estimated from the B_{2u}/B_{3u} frequency ratio, and 100° is found for the appropriate mode assignments. For a Mn−O bond length of 2.0 Å (just longer than the 1.78 Å diatomic value)[3] a 2.6 Å Mn−Mn distance across the ring is predicted. This short Mn−Mn distance suggests metal−metal bonding. Previously the Mn_2 molecule was described as a van der Waals dimer bound by weak magnetic interaction, and the Mn−Mn distance was estimated to be about 3.1−3.4 Å.[26−28] Recent local spin density calculations[29] predicted this distance to be 2.58 Å. The Mn−Mn bond may be stronger in $(MnO)_2$ due to the transfer of electron density from antibonding orbitals on the Mn−Mn subunit into Mn−O bonding orbitals.

The mechanism of $(MnO)_2$ formation is reaction 9, which

$$OMnO + Mn \rightarrow (MnO)_2 \tag{9}$$

occurs during deposition on the matrix surface and to a limited degree on first annealing. This mechanism is supported by the observation of only doublet isotopic structures in experiments with mechanical oxygen isotopic mixtures and the failure to observe $(MnO)_2$ in N_2O experiments with strong MnO and weak OMnO absorptions present.

A strong 538.3 cm^{-1} band was observed after deposition in nitrogen matrixes. It grew on annealing to 30 K and decreased thereafter. Isotopic substitution revealed doublet and triplet structures and the 16/18 ratio 1.0440. This ratio is slightly lower than that obtained for $(MnO)_2$ in argon, and this band is probably due to $(MnO)_2$ perturbed and possibly puckered by interaction with nitrogen.

$(O_2)MnO_2$. The sharp 974.9 and broad 1130 cm^{-1} bands increased markedly on annealing. Isotopic mixtures revealed doublet and triplet structures for the first band. For the second band a doublet was found with the mechanical mixture and the region was congested with the statistical mix. The isotopic ratios 1.0399 and 1.060 are characteristic of the $OOVO_2$ and $OOCrO_2$ molecules and the $(O_2)FeO_2$ molecule.[12,14,30−33] By comparison, the above bands are assigned to the "antisymmetric" stretching vibration of OMnO and the O−O stretching vibration of O_2 in the $(O_2)MnO_2$ molecule. The slight increase of the 16/18 ratio compared to MnO_2 indicates that the OMnO fragment is more bent. It should be mentioned that $OOVO_2$ has end-bonded coordination, while $(O_2)FeO_2$ is side-bonded. Moreover, the O−O vibration in $OOCoO_2$ was higher than this vibration in the CoOO molecule.[17] This is the main point: comparing results suggests that end-bonded $OOMO_2$ molecules should have stronger O−O stretching absorptions higher than the MOO molecules. Thus, assuming that the assignment of MnOO is correct, side-bonded coordination is proposed for (O_2)-MnO_2 as for $(O_2)FeO_2$. The antisymmetric FeO_2 stretching mode is blue shifted 23.1 cm^{-1} in $(O_2)FeO_2$, whereas the antisymmetric MnO_2 mode is blue shifted 24.9 cm^{-1} in (O_2)-MnO_2. Similar blue shifts are also observed for VO_2 and CrO_2 in the $OOVO_2$ and $OOCrO_2$ complexes.[14,33] Finally, the ESR spectrum[7] assigned earlier to MnO_4 is probably in fact due to the present $(O_2)MnO_2$ molecule, which is readily formed on association of MnO_2 and O_2, reaction 10.

$$OMnO + O_2 \rightarrow (O_2)MnO_2 \tag{10}$$

MnOMn. The sharp, weak 808.3 cm^{-1} band was observed after deposition, decreased on photolysis, and increased then decreased on annealing. It was stronger in experiments with higher Mn to O_2 concentration and with N_2O, which gave more MnO. Isotopic substitution produced doublets with both mixtures and the 16/18 ratio 1.0515. Based on the isotopic ratio, this band is assigned to the ν_3 vibration of the MnOMn molecule. The estimated valence angle lower limit is 140°, which is comparable to the analogous FeOFe molecule.[12] In nitrogen matrixes the 806.0 cm^{-1} band behaved analogously. The doublet isotopic structure and the 16/18 ratio 1.0519 are in good agreement with the argon matrix observations; thus this band is assigned to MnOMn in solid nitrogen.

$(MnO_2)_2$. The 951.4 cm^{-1} band grew markedly ($>10\times$) on annealing and, like the 974.9 cm^{-1} band, was favored at higher O_2 concentration. Isotopic substitution produced quartet and at least eight-band patterns with mechanical and statistical mixtures, respectively, and the 16/18 ratio 1.0483. The observed isotopic structure requires oxygen from two source molecules and the participation of four or more oxygen atoms. The most likely stoichiometry involves two inequivalent oxygen molecules. The molecule $OOMnO_2$ can be ruled out owing to the lack of a strong terminal O−O stretching mode like that found for the V and Cr species.[14,33] We are left with combinations of MnO_2 isomers, and the growth of $Mn(O_2)$ and demise of OMnO on annealing is a straightforward process. This molecule can

$$Mn(O_2) + OMnO + Mn(O_2)MnO_2 \tag{11}$$

explain the higher-than-diatomic isotopic ratio through interaction between symmetric stretching modes of the terminal MnO_2 and internal $Mn(O_2)$ subunits. This aggregate molecule is probably nonplanar.

The 850.7 and 847.7 cm^{-1} bands, like the 808.3 cm^{-1} band, are favored at higher Mn to O_2 ratios, which suggests more than one Mn atom, and they decrease on photolysis but grow back on annealing. These bands show evidence of secondary isotopic splitting. The 847.3 cm^{-1} band gives a pure isotopic doublet with the mechanical mix, indicating one dioxygen unit, and a quartet with the statistical mix, revealing inequivalent atomic positions. These observations identify MnOMnO and suggest that a second Mn atom adds to bent OMnO. The 847.3 cm^{-1} band is best assigned to a bent MnOMnO molecule. The 850.7 cm^{-1} band is due to a similar molecule tentatively identified as OMnOMnO. The analogous nickel oxide species were observed, where nickel isotopic splittings gave evidence of two Ni atoms.[18]

Other Absorptions. A number of other absorptions appear on annealing in these experiments. Although some of these bands are sharp and clear, oxygen-18 shifts are observed; typically the mixed isotopic counterparts required for identification are masked by other absorptions or are too weak to be observed. These aggregate products, noted Mn_xO_y in Table 1, cannot be identified here. Finally, two weak bands that appear at 778 and 772 cm^{-1} on 35−40 K annealing in the 1% O_2 experiments may be due to the strongest absorption[10] of Mn_2O_7.

Conclusions

Laser-ablated Mn atoms react with O_2 to give MnO, OMnO, $(MnO)_2$, and MnO_2^- as major products, which are identified from oxygen isotopic substitution. Annealing allows further association to form the cyclic $Mn(O_2)$ complex, the higher oxides Mn_2O_2 and Mn_2O_3, and the $(O_2)MnO$ and $(O_2)MnO_2$ oxide complexes, which are analogous to the $(O_2)FeO$ and $(O_2)FeO_2$ complexes. The MnO molecule is observed at 833.1 cm^{-1}, just 3.1 cm^{-1} above the gas-phase fundamental. The OMnO molecule is bent based on the observation of both ν_3 and DFT calculations; the oxygen-18 shift for ν_3 provides a valence angle determination of 135 ± 5°. It appears that metastable excited states contribute to the reactivity of laser-ablated Mn atoms. The cyclic $Mn(O_2)$ molecule formed, on association of cold reagents, involves a weaker bonding interaction than the cyclic $Fe(O_2)$ molecule. The short 2.6 Å estimated Mn−Mn distance across the rhombic $(MnO)_2$ ring is compatible with substantial metal−metal bonding.

References and Notes

(1) Bagus, P. S.; Freund, H. J.; Minerva, T.; Pacchioni, G.; Parmigiani, F. *Chem. Phys. Lett.* **1996**, *251*, 90, and references therein.

(2) Vanelo, J.; Patze, R. H.; Eskes, H.; Berger, R.; Sawatzky, G. A. *Phys. Rev. B: Condens. Matter* **1991**, *44*, 1530.

(3) Huber, K. P.; Herzberg, G. *Constants of Diatomic Molecules*; Van Nostrand: New York, 1979. Krasnov, K. S. *Molecular Constants of Inorganic Compounds*; Khimia: Leningrad, 1979.

(4) Gordon, R. M.; Merer, A. J. *Can. J. Phys.* **1980**, *58*, 642.

(5) Adams, A. G.; Azuma, Y.; Li, H.; Merer, A. J.; Chandrakumar, T. *Chem. Phys.* **1991**, *152*, 391.

(6) Bauschlicher, C. W., Jr.; Maitre, P. *Theor. Chim. Acta* **1995**, *90*, 189.

(7) Ferrante, R. F.; Wilkerson, J. L.; Graham, W. R. M.; Weltner, W., Jr. *J. Chem. Phys.* **1977**, *67*, 5904.

(8) Serebrennikov, L. V.; Maltsev, A. A. *Vestn. Mosk. Univ. Ser. 2, Khim.* **1980**, *2*, 148.

(9) Serebrennikov, L. V. Dr. of Sci. Thesis, Moscow State University, Moscow, 1990.

(10) Levason, W.; Ogden, J. S.; Turff, J. W. *J. Chem. Soc., Dalton Trans.* **1983**, 2699.

(11) Almond, M. J. *J. Mol. Struct.* **1988**, *172*, 157.

(12) Chertihin, G. V.; Saffel, W.; Yustein, J. T.; Andrews, L.; Neurock, M.; Ricca, A.; Bauschlicher, C. E., Jr. *J. Phys. Chem.* **1996**, *100*, 5261.

(13) Levy, M. R. *J. Phys. Chem.* **1989**, *93*, 5195.

(14) Chertihin, G. V.; Bare, W. D.; Andrews, L. *J. Chem. Phys.* **1997**, *107*, 2798.

(15) Frisch, M. J.; Trucks, G. W.; Schlegel, H. B.; Gill, P. M. W.; Johnson, B. G.; Robb, M. A.; Cheeseman, J. R.; Keith, T.; Petersson, G. A.; Montgomery, J. A.; Raghavachari, K.; Al-Laham, M. A.; Zakrzewski, V. G.; Ortiz, J. V.; Foresman, J. B.; Cioslowski, J.; Stefanov, B. B.; Nanayakkara, A.; Challacombe, M.; Peng, C. Y.; Ayala, P. Y.; Chen, W.; Wong, M. W.; Andres, J. L.; Replogle, E. S.; Gomperts, R.; Martin, R. L.; Fox, D. J.; Binkley, J. S.; Defrees, D. J.; Baker, J.; Stewart, J. P.; Head-Gordon, M.; Gonzalez, C.; Pople J. A. *Gaussian 94, Revision B.1*; Gaussian, Inc.: Pittsburgh, PA, 1995.

(16) Green, D. W.; Reedy, G. T.; Kay, J. G. *J. Mol. Spectrosc.* **1979**, *78*, 257.

(17) Chertihin, G. V.; Citra, A.; Andrews, L.; Bauschlicher, C. W., Jr. *J. Phys. Chem. A*, in press.

(18) Citra, A.; Chertihin, G. V.; Andrews, L.; Neurock, M. *J. Phys. Chem. A* **1997**, *101*, 3109.

(19) Andrews, L.; Chertihin, G. V.; Citra, A.; Neurock, M. *J. Phys. Chem.* **1996**, *100*, 11235.

(20) Kauffman, J. W.; Hauge, R. H.; Margrave, J. L. *J. Phys. Chem.* **1985** *89*, 3541.

(21) Chertihin, G. V.; Rojanskii, I. L.; Serebrennikov, L. V.; Shevelkov, V. F. *Vestn. Mosk. Univ. Ser. 2, Khim.*, Deposit VINITI N9034-B85, 1985.

(22) Chertihin, G. V., Ph.D. Thesis, Moscow State University, Moscow, 1987.

(23) Rubinovitz, R. L.; Nixon, E. R. *J. Phys. Chem.* **1986**, *90*, 1940.

(24) Andrews, L. *J. Chem. Phys.* **1969**, *50*, 4288.

(25) Chertihin, G. V.; Andrews, L. *J. Chem. Phys.* **1996** *105*, 2561.

(26) Baumann, C. A.; Van Zee, R. J.; Bhat, C. V.; Weltner, W., Jr. *J. Chem. Phys.* **1983**, *78*, 190.

(27) Cheeseman, M.; Van Zee, R. J.; Weltner, W., Jr. *J. Chem. Phys.* **1989**, *91*, 2748.

(28) Moskovits, M.; DiLella, D. P.; Limm, W. *J. Chem. Phys.* **1984**, *80*, 626.

(29) Piechota, J.; Suffczynski, M. *Int. J. Mod. Phys. B.* **1993**, *7*, 560.

(30) Poliakoff, M.; Smith, K. P.; Turner, J.; Wilkinson, A. J. *J. Chem. Soc., Dalton. Trans.* **1982**, 651.

(31) Almond, M. J.; Downs, A. J.; Perutz, R. N. *Inorg. Chem.* **1985**, *24*, 275.

(32) Almond, M. J.; Hahne, M. *J. Chem. Soc., Dalton. Trans.* **1988**, 2255.

(33) Chertihin, G. V.; Bare, W. D.; Andrews, L. *J. Phys. Chem. A* **1997**, *101*, 5090.